Development 139, 1071-1082 (2012) doi:10.1242/dev.069070

The role of Hes genes in intestinal development, homeostasis and tumor formation

Taro Ueo[1,2], Itaru Imayoshi[2,3], Taeko Kobayashi[2,4], Toshiyuki Ohtsuka[2,4], Hiroshi Seno[1], Hiroshi Nakase[1], Tsutomu Chiba[1] and Ryoichiro Kageyama[2,4,*]

SUMMARY

Notch signaling regulates intestinal development, homeostasis and tumorigenesis, but its precise downstream mechanism remains largely unknown. Here we found that inactivation of the Notch effectors *Hes1*, *Hes3* and *Hes5*, but not *Hes1* alone, led to reduced cell proliferation, increased secretory cell formation and altered intestinal structures in adult mice. However, in *Apc* mutation-induced intestinal tumors, inactivation of *Hes1* alone was sufficient for reducing tumor cell proliferation and inducing differentiation of tumor cells into all types of intestinal epithelial cells, but without affecting the homeostasis of normal crypts owing to genetic redundancy. These results indicated that Hes genes cooperatively regulate intestinal development and homeostasis and raised the possibility that Hes1 is a promising target to induce the differentiation of tumor cells.

KEY WORDS: Hes, Notch signaling, Intestinal tumor, Intestine, Stem cell, Mouse

INTRODUCTION

The intestinal epithelium is shaped into crypts, which are invagination structures, and villi, which are finger-like protrusions, and is continuously renewed from stem cells throughout life (Radtke and Clevers, 2005; Crosnier et al., 2006; Scoville et al., 2008). Stem cells are located at the bottom of the crypts and produce transit-amplifying progenitors, which then undergo terminal differentiation into four distinct cell types: absorptive cells, mucin-secreting goblet cells, anti-bacterial peptide-secreting Paneth cells, and gut hormone-secreting enteroendocrine cells. The latter three cell types belong to the secretory cell lineage. Postmitotic differentiated cells migrate towards the apex of a villus before being shed into the intestinal lumen. It has been shown that signaling molecules such as those of the Notch signaling pathway are involved in the homeostasis of the intestinal cellular system, including stem cell maintenance, cell fate decision and maturation (Radtke and Clevers, 2005; Crosnier et al., 2006; Scoville et al., 2008), but the precise downstream mechanisms and crosstalk of signaling pathways remain to be determined.

It has been shown that the Notch signaling pathway is also involved in the development of colorectal tumors. In Apc^{Min} mice, the Wnt signaling effector β-catenin is stabilized by mutations in the intestinal tumor suppressor gene *Apc*, and β-catenin forms a complex with Tcf factors in the nucleus, which causes continuous expression of Wnt target genes and the development of adenomas, mainly in the small intestine (Moser et al., 1990; Su et al., 1992; Bienz and Clevers, 2000; van de Wetering et al., 2002). However, blockade of Notch signaling with a γ-secretase inhibitor turned adenoma cells of Apc^{Min} mice into goblet cells (van Es et al., 2005a), whereas activation of Notch signaling in *Apc* mutant ($Apc^{+/1638N}$) mice resulted in at least a 20-fold increase in the number of adenoma cells compared with that in $Apc^{+/1638N}$ mice (Fre et al., 2009), suggesting that Notch signaling is involved in intestinal tumor formation. Although Notch signaling is a promising target for anti-cancer therapy, all stem/progenitor cells in healthy intestinal regions, as well as the tumor cells, differentiate into goblet cells by inhibition of Notch signaling, which could cause severe side effects. Thus, a strategy to inhibit Notch signaling only in tumor cells without affecting healthy cells is desirable.

Notch signaling is conveyed from cell to cell (Wilson and Radtke, 2006; Kageyama et al., 2007). When the membrane-bound Notch receptor interacts with its ligand anchored in the membrane of neighboring cells, an intrinsic γ-secretase cleaves the receptor, releasing the Notch intracellular domain (NICD). NICD then translocates into the nucleus where it forms an active transcriptional complex with Rbpj, an essential mediator of all Notch receptors, to stimulate the expression of many target genes. *Hes1*, one of the best-characterized target genes of the Notch signaling pathway, regulates the maintenance of neural and hematopoietic stem cells (Ohtsuka et al., 1999; Kunisato et al., 2003; Shimojo et al., 2008). It has been shown that Hes1 is expressed by proliferating cells, including stem cells in the intestinal crypt, and that it represses the expression of the *Math1* (*Atoh1*) and neurogenin 3 (*Ngn3* or *Neurog3*) genes (Jensen et al., 2000; Yang et al., 2001; Jenny et al., 2002; Kayahara et al., 2003; Fre et al., 2005; van Es et al., 2005a; Suzuki et al., 2005; Riccio et al., 2008; Kopinke et al., 2011). *Math1* regulates the development of all types of secretory cells, whereas *Ngn3* regulates enteroendocrine cell development (Yang et al., 2001; Jenny et al., 2002). Transgenic mice expressing NICD constitutively upregulate Hes1 expression, increase the number of proliferating cells and lose all secretory cells, whereas *Hes1* knockout (KO) mice show overproduction of secretory cells (Jensen et al., 2000; Stanger et al., 2005). These results suggest that the Notch-Hes1 pathway promotes the proliferation of intestinal stem/progenitor cells and inhibits secretory cell development by repressing *Math1* and *Ngn3* expression. Hes1 is also expressed in human colon cancer cells and in adenoma cells of Apc^{Min} mice (van Es et al., 2005a; Fernández-

[1]Department of Gastroenterology and Hepatology, Kyoto University Graduate School of Medicine, Kyoto 606-8501, Japan. [2]Institute for Virus Research, Kyoto University, Kyoto 606-8507, Japan. [3]Japan Science and Technology Agency, PRESTO, Kyoto 606-8507, Japan. [4]Japan Science and Technology Agency, CREST, Kyoto 606-8507, Japan.

*Author for correspondence (rkageyam@virus.kyoto-u.ac.jp)

Accepted 9 January 2012

Majada et al., 2007), and *Hes1* functions as a downstream target of both the Notch and Wnt signaling pathways in Ls174T colon cancer cells (Rodilla et al., 2009), suggesting that crosstalk between Notch and Wnt signaling might take place via Hes1. In the absence of *Hes1*, *Hes3* and *Hes5* expression is upregulated in the intestine (Jensen et al., 2000), but it remains unclear whether all Hes genes function similarly or whether *Hes1* has a dominant role in intestinal development, homeostasis and tumor formation.

In order to determine the roles of Hes genes in postnatal intestinal development, homeostasis and tumor formation, we analyzed the intestine of *Hes1* conditional KO (cKO) and *Hes1/Hes3/Hes5* (*Hes1/3/5*) cKO mice and crossed these mice with Apc^{Min} mice to determine the roles of Hes genes in intestinal tumors.

MATERIALS AND METHODS

Mice

Villin-Cre mice (el Marjou et al., 2004) and Apc^{Min} mice (Su et al., 1992) were obtained from Jackson Laboratories. *Hes1* cKO mice were generated by crossing homozygous *Hes1* floxed mice (Imayoshi et al., 2008) with *Villin-Cre*;$Hes1^{+/-}$ mice. *Hes1/3/5* cKO mice were generated by crossing $Hes1^{flox/flox}$;$Hes3^{-/-}$;$Hes5^{-/-}$ with *Villin-Cre*;$Hes1^{+/-}$;$Hes3^{-/-}$;$Hes5^{-/-}$. *Villin-Cre*;$Hes1^{flox/+}$ and *Villin-Cre*;$Hes1^{flox/+}$;$Hes3^{-/-}$;$Hes5^{-/-}$ mice were normal and used as controls. Apc^{Min};*Hes1* cKO mice were obtained by crossing homozygous *Hes1* floxed mice with Apc^{Min};*Villin-Cre*;$Hes1^{+/-}$ mice.

Ah-Cre mice were generated as previously reported (Campbell et al., 1996; Ireland et al., 2004). The plasmid pAHIR1 was kindly gifted by Dr C. Roland Wolf (Dundee, UK). Rosa-lacZ mice (Soriano, 1999) were kindly supplied by Dr Philippe Soriano. Apc^{Min};*Ah-Cre*;$Hes1^{flox/-}$ mice were obtained by crossing homozygous *Hes1* floxed mice with Apc^{Min};*Ah-Cre*;$Hes1^{+/-}$ mice. For induction of the *Ah* promoter, mice were treated with 80 μg/g body weight β-naphthoflavone in corn oil by intraperitoneal injection for 5 consecutive days and sacrificed after 3 weeks. All animals were handled in accordance with the Kyoto University Guide for the Care and Use of Laboratory Animals.

Histology and immunohistochemistry

Tissues were fixed overnight in 10% neutral buffered formalin, paraffin embedded and sectioned at 3-5 μm. Sections were stained with Hematoxylin and Eosin or Alcian Blue or subjected to immunohistochemistry with the following primary antibodies: anti-cleaved caspase 3 (1:200 dilution, Cell Signaling), anti-BrdU (1:500, BD), anti-Hes1 (1:100), anti-Hes3 (1:100, Santa Cruz), anti-Hes5 (1:100, Abcam), anti-Ki67 (1:100, DAKO), anti-lysozyme (1:200, DAKO), anti-villin (1:100, Cell Signaling), anti-chromogranin (1:100, DiaSorin, Stillwater, MN, USA), anti-Lgr5 (1:300, MBL International), anti-β-catenin (1:50, Transduction Laboratories), anti-EphB3 (1:50, R&D Systems), anti-phosphorylated Smad1/5/8 (1:200, Cell Signaling), anti-Math1 (1:50, Development Studies Hybridoma Bank), anti-Ngn3 (1:300, Development Studies Hybridoma Bank) and anti-Sox9 (1:1000, Chemicon). Antigen retrieval was performed by boiling in 10 mM citrate buffer pH 6.0 for 15 minutes for all antibodies except anti-lysozyme, which was used after treatment with 20 μg/ml proteinase K in TE pH 8.0 (10 minutes at 37°C), and anti-BrdU, which was used after treatment with 2 N HCl (30 minutes at 37°C) and boiling in citrate buffer as above. Immunoperoxidase labeling was performed with the VECTASTAIN ABC Kit (Vector Laboratories). Slides were developed using DAB and counterstained with Hematoxylin.

For X-gal staining, perfusion with 4% paraformaldehyde in 0.1 M phosphate buffer was performed, and frozen sections (8 μm) were prepared. These sections were stained with X-gal as previously described (Imayoshi et al., 2006). For single BrdU labeling, mice were injected intraperitoneally with 100 mg/kg BrdU 2, 48 or 96 hours before sacrifice. For multiple BrdU labeling, mice were injected intraperitoneally with 100 mg/kg BrdU four times at 2-hour intervals and sacrificed after 9 days.

For quantification, the number of each cell type per section was counted in at least five sections of three animals per genotype. Statistical differences were determined by Student's *t*-test.

RESULTS

Accelerated differentiation of secretory cells in the small intestine of *Hes1* cKO mice at a postnatal stage

Because *Hes1* KO mice die soon after birth (Ishibashi et al., 1995), the postnatal role of *Hes1* was not known. To understand the role of *Hes1* in postnatal development and homeostasis of the intestine, we generated *Hes1* cKO mice by crossing *Hes1* flox mice (Imayoshi et al., 2008) with Villin-Cre mice, which induced a Cre-dependent recombination in the intestinal epithelium by embryonic day (E) 12.5 (Madison et al., 2002; el Marjou et al., 2004). In *Villin-Cre*;$Hes1^{flox/-}$ mice, Hes1 was almost completely ablated and Hes1 expression was not detectable in the intestinal epithelium (supplementary material Fig. S1A-F,S,T). Therefore, these mutants were used as *Hes1* cKO mice. *Villin-Cre*;$Hes1^{flox/+}$ mice were apparently normal and were used as controls.

Hes1 cKO mice were born at the expected frequency and survived throughout adulthood. On postnatal day (P) 2.5, the crypt-villus structure of the small intestine was apparently normal (Fig. 1A,B) and the numbers of proliferating cells ($Ki67^+$) and absorptive cells ($villin^+$) were unchanged in *Hes1* cKO mice compared with controls (Fig. 1C-F). However, the numbers of apoptotic cells (cleaved caspase 3^+), goblet cells (Alcian $Blue^+$) and enteroendocrine cells ($chromogranin^+$) were noticeably increased in *Hes1* cKO mice (Fig. 1G-L,O-Q). Normally, Paneth cells ($lysozyme^+$) appear 2 weeks after birth, and they were not detectable in control mice at this stage (Fig. 1M). In *Hes1* cKO mice, Paneth cells were largely absent at this stage (Fig. 1N), although a very small number were prematurely differentiated (Suzuki et al., 2005). Thus, *Hes1* seems to be important for generation of the correct number of intestinal cells and for their survival. However, at 2 months of age, these defects were not observed in *Hes1* cKO mice (supplementary material Fig. S2), suggesting that *Hes1* deficiency was mostly compensated in the adult.

Accelerated differentiation of secretory cells in the small intestine of *Hes1/3/5* cKO mice at postnatal and adult stages

It was previously shown that, in the absence of *Hes1*, the related genes *Hes3* and *Hes5* are upregulated in the embryonic intestine (Jensen et al., 2000). This was confirmed in the postnatal *Hes1* cKO mice (supplementary material Fig. S1O-R), suggesting that *Hes3* and *Hes5* compensate for a *Hes1* deficiency. To examine this possibility, we generated *Villin-Cre*;$Hes1^{flox/-}$;$Hes3^{-/-}$;$Hes5^{-/-}$ (*Hes1/3/5* cKO) mice (supplementary material Fig. S1G-N). $Hes3^{-/-}$;$Hes5^{-/-}$ (*Hes3/5* KO) mice (Hatakeyama et al., 2004) and *Villin-Cre*;$Hes1^{flox/+}$;$Hes3^{-/-}$;$Hes5^{-/-}$ mice were apparently normal and were used as controls. Hes1 is expressed by proliferating cells but not by Paneth cells in controls (supplementary material Fig. S1D, red arrows), whereas Hes5 is normally expressed by Paneth cells (van Es et al., 2005a). However, Hes1 was expressed by Paneth cells in *Hes3/5* KO mice (supplementary material Fig. S1H, red arrows), suggesting that *Hes1* compensates for *Hes3* and *Hes5* deficiency.

In *Hes1/3/5* cKO mice, the histological structure of the small intestine was apparently normal (Fig. 2A,B) and absorptive cells ($villin^+$) were not affected at P2.5 (Fig. 2C,D). However, the numbers of goblet cells (Alcian $Blue^+$) and enteroendocrine cells ($chromogranin^+$) were increased in *Hes1/3/5* cKO mice at P2.5 (Fig. 2E-H,P,Q), as observed in *Hes1* cKO mice. Furthermore,

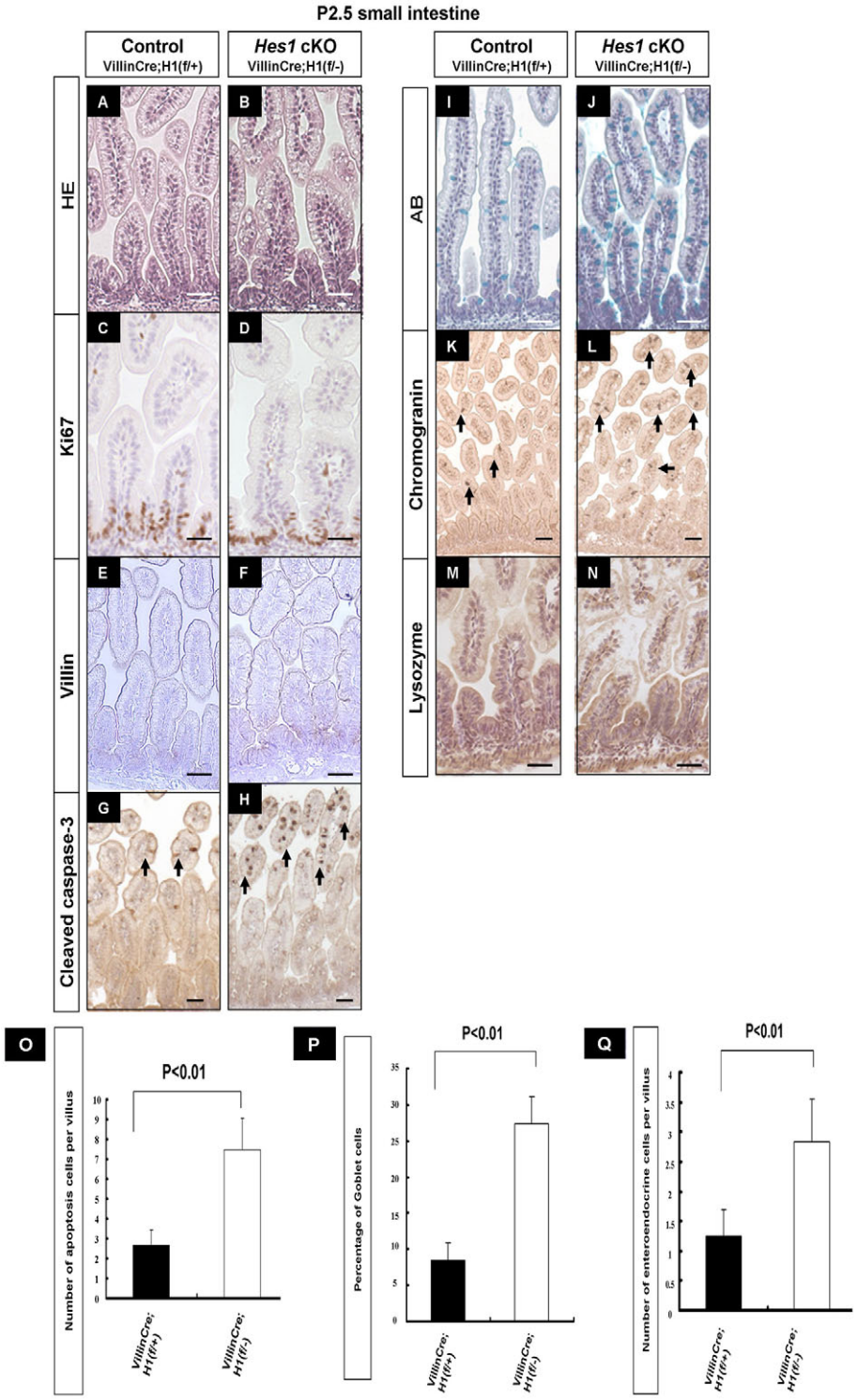

Fig. 1. Defects in the small intestine of *Hes1* cKO mice at P2.5. The small intestines of *Hes1* cKO and control mice were examined at P2.5. (**A**,**B**) Hematoxylin-Eosin staining showing that the gross structure of the small intestine of *Hes1* cKO mice (B) was unaffected compared with controls (A). (**C-F**) The numbers of Ki67$^+$ proliferating cells (C,D) or villin$^+$ absorptive cells (E,F) were unchanged in *Hes1* cKO mice. (**G**,**H**) The number of cleaved caspase 3$^+$ apoptotic cells (some are indicated by arrows) was increased in *Hes1* cKO mice. (**I**,**J**) Alcian Blue (AB) staining showed an increased number of goblet cells in *Hes1* cKO mice. (**K**,**L**) The number of chromogranin$^+$ enteroendocrine cells (some are indicated by arrows) was increased in *Hes1* cKO mice. (**M**,**N**) Lysozyme$^+$ Paneth cells were not detectable in these sections. Scale bars: 100 μm. (**O-Q**) Quantification of the number of apoptotic (O), goblet (P) and enteroendocrine (Q) cells. Error bars indicate s.d.

Paneth cells (lysozyme$^+$) were prematurely differentiated in *Hes1/3/5* cKO mice at P2.5, whereas they were not present in controls (Fig. 2I,J,R). Interestingly, some of these prematurely differentiated Paneth cells did not remain at the intervillus pocket but moved upwards along the crypt-villus axis (Fig. 2J). Furthermore, the number of apoptotic cells was increased in *Hes1/3/5* cKO mice (Fig. 2K,L, arrows, Fig. 2S). Thus, Hes genes are required for the proper differentiation of secretory cells and for the survival of intestinal cells.

Proliferating cells were present at the intervillus pocket as well as in the upper region in controls, whereas they were absent from the intervillus pocket in *Hes1/3/5* cKO mice but present in the upper region (Fig. 2M,N). Quantification indicated that the number of proliferating cells at P2.5 was reduced in *Hes1/3/5* cKO mice compared with controls (Fig. 2O). Similar defects were observed in *Hes1/3/5* cKO mice at 2 months of age (supplementary material Fig. S3). At this age, crypt base columnar (CBC) cells, which constitute actively cycling Ki67$^+$ Lgr5$^+$ stem cells (Barker et al., 2007), resided

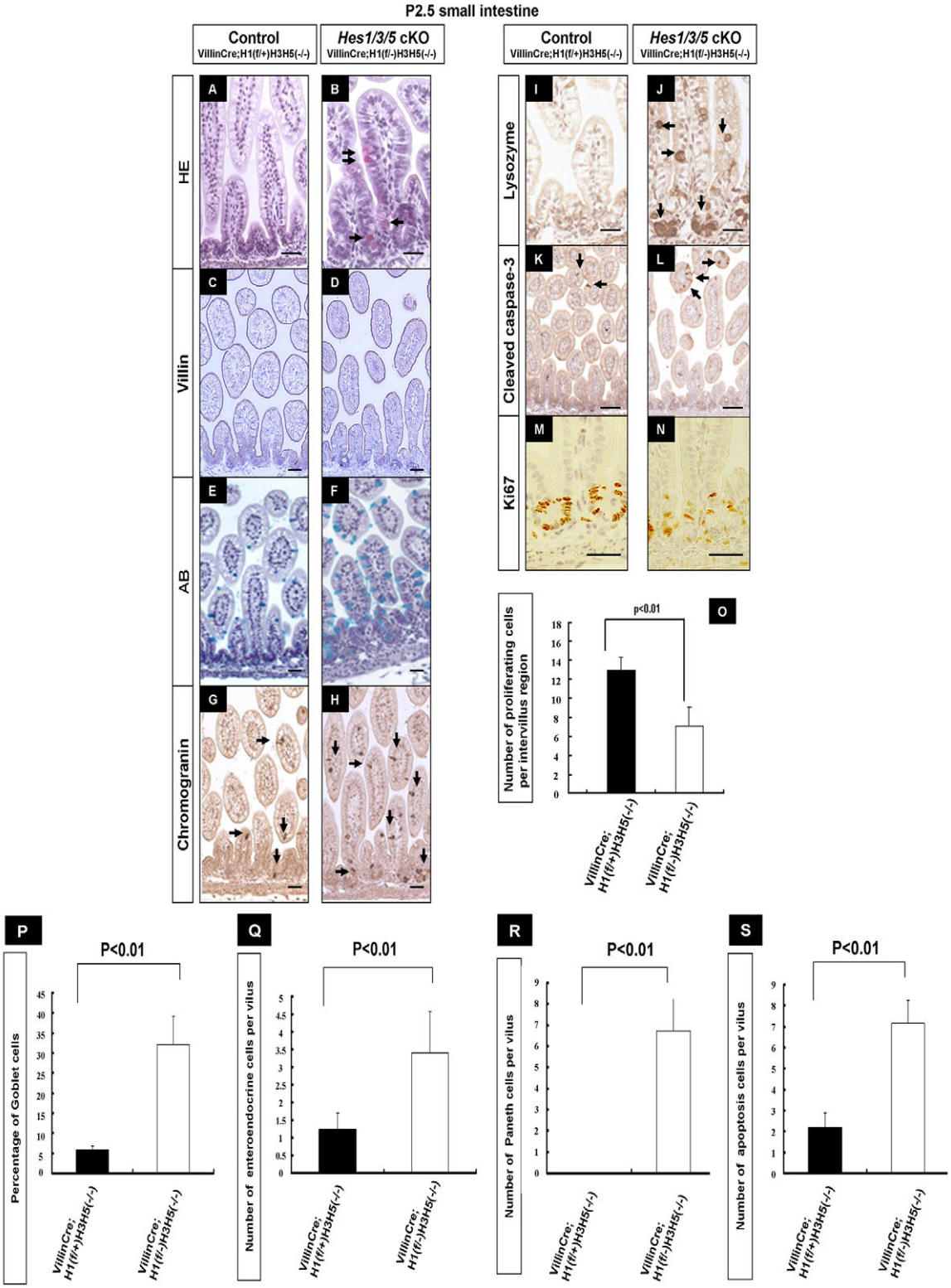

Fig. 2. Defects in the small intestine of *Hes1/3/5* cKO mice at P2.5. The small intestines of *Hes1/3/5* cKO and control mice were examined at P2.5. (**A**,**B**) Hematoxylin-Eosin staining showing that the gross structure of the small intestine of *Hes1/3/5* cKO mice (B) was unaffected compared with controls (A). (**C**,**D**) The development of villin^{+} absorptive cells was not disturbed in *Hes1/3/5* cKO mice. (**E-H**) In *Hes1/3/5* cKO mice, the numbers of goblet cells (E,F) and enteroendocrine cells (G,H) were increased. (**I**,**J**) In control mice, Paneth cells were not observed (A,I), but in *Hes1/3/5* cKO mice Paneth cells were present (B,J, arrows). Some Paneth cells did not remain in the intervillus pockets but migrated towards the top of the villi. (**K**,**L**) The number of apoptotic cells (arrows) was increased in *Hes1/3/5* cKO mice. (**M**,**N**) The number of Ki67^{+} proliferating cells was decreased in *Hes1/3/5* cKO mice, and these cells were absent from the intervillus pocket (N), although they were present at the intervillus pocket in control mice (M). Scale bars: 100 μm. (**O**) The number of proliferating cells per intervillus region was reduced in *Hes1/3/5* cKO mice. (**P-S**) Quantification of the number of goblet (P), enteroendocrine (Q), Paneth (R) and apoptotic (S) cells. Error bars indicate s.d.

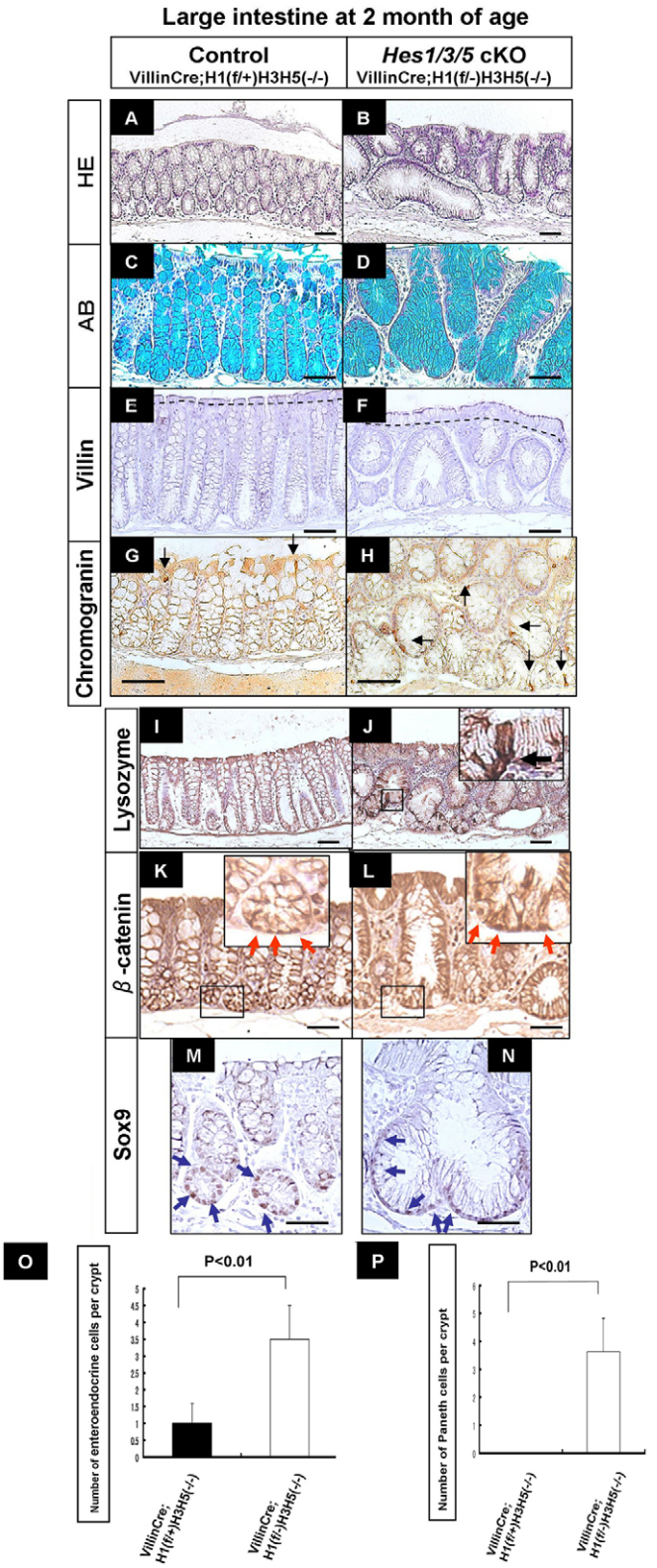

Fig. 3. Defects in the large intestine of *Hes1/3/5* cKO mice at 2 months of age. The large intestines of 2-month-old *Hes1/3/5* cKO and control mice were examined. (**A**,**B**) Hematoxylin-Eosin staining showed that crypts of the large intestine were expanded in *Hes1/3/5* cKO mice (B) as compared with controls (A). (**C**,**D**) Alcian Blue staining showed that the dominant cell population of the epithelium was goblet cells in both *Hes1/3/5* cKO and control mice. (**E-N**) Immunohistochemical staining for villin (E,F), chromogranin (G,H, arrows), lysozyme (I,J), β-catenin (K,L) and Sox9 (M,N, arrows). Absorptive cell differentiation was not altered (E,F, above dashed line). Paneth cells (lysozyme^{+}) were not present in the large intestine of control mice (I), but many were present in *Hes1/3/5* cKO mice (J, arrow in inset). Scale bars: 100 μm. (**O**,**P**) Quantification of the number of enteroendocrine (O) and Paneth (P) cells. Error bars indicate s.d.

between Paneth cells at the crypt bottom in controls (supplementary material Fig. S3I,K, black and red arrows). In *Hes1/3/5* cKO mice, however, CBC cells were not present at the crypt bottom, but were located away from this region, although their number was not noticeably changed (supplementary material Fig. S3J,L,N, arrows). These results suggest that, in the absence of Hes genes, cell proliferation is reduced, although stem cells are well maintained.

The above data also indicate that whereas differentiation of secretory cells was exclusively inhibited by *Hes1* at a neonatal stage, it was cooperatively inhibited by *Hes1*, *Hes3* and *Hes5* in order to maintain adult homeostasis. It has been shown that differentiation of secretory cells is regulated by *Math1* and *Ngn3* (Yang et al., 2001; Jenny et al., 2002), so we examined *Math1* and *Ngn3* expression in *Hes1/3/5* cKO mice. Immunohistochemical analysis showed that Math1 and Ngn3 expression was upregulated in the small intestine of *Hes1/3/5* cKO mice (supplementary material Fig. S4, black and red arrows). Thus, we conclude that Hes genes inhibit the differentiation of secretory cells by repressing *Math1* and *Ngn3* expression.

In control mice, Paneth cells remained at the crypt bottom and expressed nuclear β-catenin, an active Wnt signaling effector (supplementary material Fig. S5C,D, arrows). These cells also expressed EphB3, a downstream target of Wnt signaling, which determines the position of Paneth cells (supplementary material Fig. S5E, arrows) (Batlle et al., 2002). In *Hes1/3/5* cKO adult mice, however, many Paneth cells moved away from the crypt bottom (supplementary material Fig. S5F, red arrows), and these mispositioned Paneth cells expressed neither nuclear β-catenin nor EphB3 (supplementary material Fig. S5F-H, red arrows), suggesting that these Paneth cells failed to undergo Wnt-dependent maturation.

Abnormal structures and enhanced secretory cell differentiation in the large intestine of Hes mutant mice

We next examined the large intestine of *Hes1* cKO and *Hes1/3/5* cKO mice. Compared with control mice, the crypts of the large intestine of *Hes1* cKO mice were greatly expanded, and proliferating cells were mispositioned in *Hes1* cKO mice at P16 (supplementary material Fig. S6A-D). Furthermore, although Paneth cells (lysozyme^{+}) were not observed in the large intestine of control mice, they appeared ectopically in *Hes1* cKO mice (supplementary material Fig. S6E,F, arrows). However, these defects were not observed in *Hes1* cKO mice at 2 months of age (supplementary material Fig. S6G-J), suggesting that *Hes3* and *Hes5* compensate for *Hes1* deficiency. In agreement with this notion, crypts of the large intestine were greatly expanded in *Hes1/3/5* cKO mice even at 2 months of age (Fig. 3A,B). The dominant population of the epithelial cells were goblet cells in both control and *Hes1/3/5* cKO mice (Fig. 3C,D), and no apparent abnormality was observed in absorptive cells of the mutants (Fig. 3E,F, above dashed line). In addition, cells in the crypt base

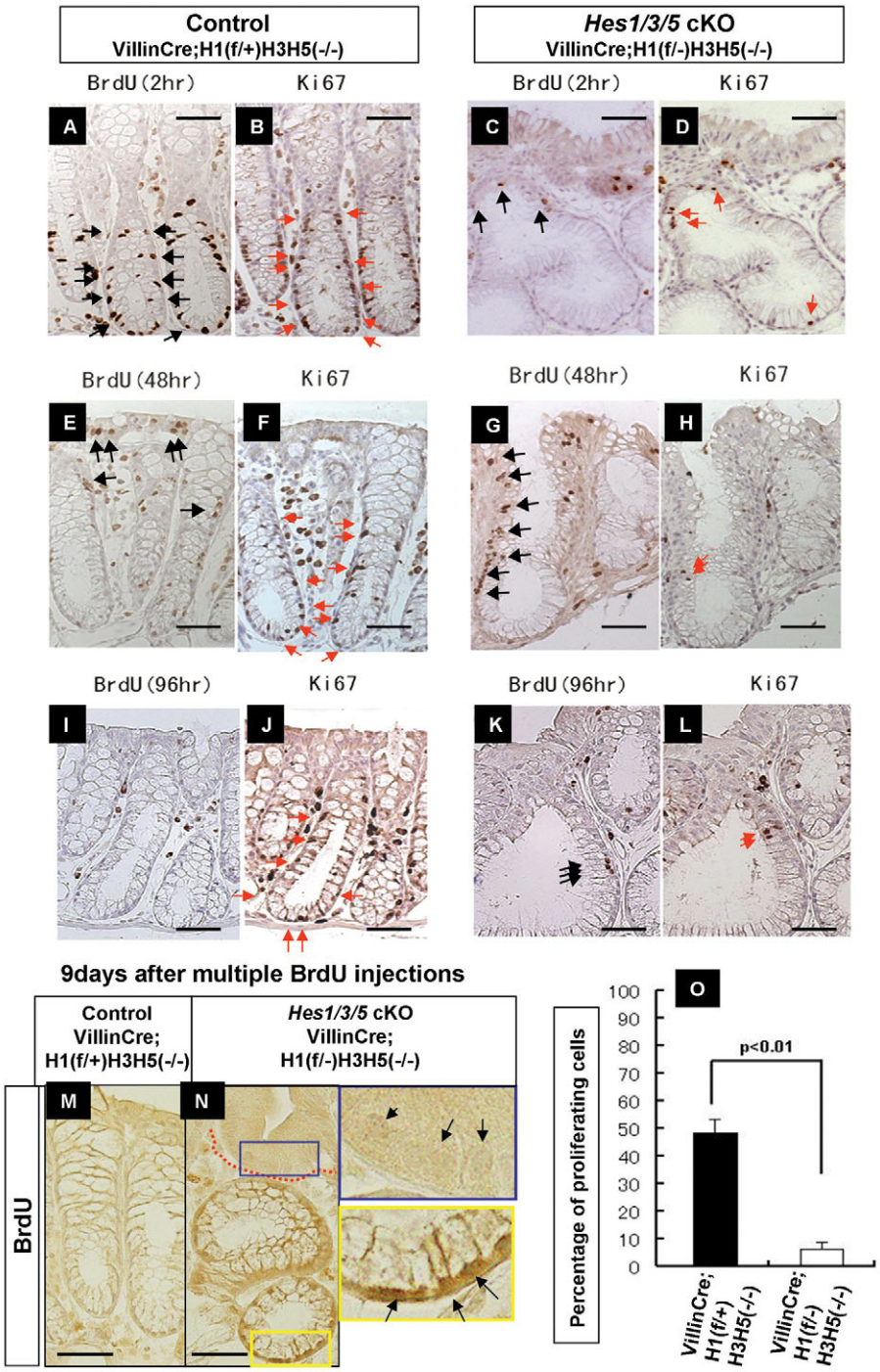

Fig. 4. Defects in cell proliferation and migration in the large intestine of *Hes1/3/5* cKO mice. Cell proliferation and migration in the large intestines of *Hes1/3/5* cKO and control mice were examined at 2 months of age. (**A-L**) Immunohistochemical analysis of BrdU uptake (A,C,E,G,I,K) and Ki67 (B,D,F,H,J,L). Mice were sacrificed 2 (A-D), 48 (E-H) or 96 (I-L) hours after a single BrdU injection. BrdU and Ki67 were examined in neighboring sections. In controls, many proliferating cells were present within the bottom two-thirds of the crypt (B,F,J, arrows). Two hours after BrdU administration, all BrdU$^+$ cells existed within the bottom two-thirds of the crypt in controls (A, arrows). Forty-eight hours later, BrdU$^+$ cells migrated (E, arrows) and had mostly disappeared 96 hours later (I). In *Hes1/3/5* cKO mice, the number of proliferating cells decreased and they were present in the middle region of crypts (D,H,L, arrows). BrdU$^+$ cells were initially present in the middle region of crypts (C, arrows) but then migrated to both the luminal and bottom sides (G, arrows). After 96 hours, BrdU$^+$ cells that had migrated to the luminal side disappeared, whereas those that had migrated to the bottom side still remained in crypts (K, arrows). (**M**,**N**) The turnover of differentiated cells of control (M) and *Hes1/3/5* cKO (N) mice was examined by multiple BrdU injections. Nine days after multiple BrdU injections, no BrdU$^+$ cells were detectable in the large intestine of control mice (M), whereas many BrdU$^+$ cells were observed in the cystic crypt bottom (N, below dotted red line, arrows in yellow inset) but not in the luminal side (arrows in blue inset). Scale bars: 100 μm. (**O**) Quantification of the number of proliferating cells. Error bars indicate s.d.

expressed nuclear β-catenin similarly in control and *Hes1/3/5* cKO mice (Fig. 3K,L, arrowheads in insets). However, the number of enteroendocrine cells was increased in *Hes1/3/5* cKO mice (Fig. 3G,H,O). Furthermore, Paneth cells were formed ectopically in *Hes1/3/5* cKO mice at 2 months of age (Fig. 3I,J, arrows, Fig. 3P).

Abnormal cell proliferation and migration in the large intestine of Hes mutant mice

We next examined the proliferation and migration of cells of the large intestine in mutant and control mice at 2 months of age by administration of BrdU and performing immunohistochemistry for Ki67. Two hours after BrdU administration, all BrdU$^+$ cells were present within the bottom two-thirds of the crypt in controls (Fig. 4A), and Ki67$^+$ cells were also found in the same region (Fig. 4B,F,J, arrows), indicating that cell proliferation occurs within the bottom two-thirds of the crypt. Lgr5$^+$ stem cells also resided at the crypt bottom (supplementary material Fig. S7A, arrows). After a period of 48 hours, BrdU was not retained by proliferating cells (Ki67$^+$) but by cells that exited the cell cycle soon after BrdU administration. At this stage, these BrdU$^+$ cells migrated upwards (Fig. 4E, arrows) and had mostly disappeared 96 hours later in the controls (Fig. 4I). In *Hes1/3/5* cKO mice, however, the number of proliferating cells was much reduced, and most remained around the middle region of expanded crypts (Fig. 4C,D,H,L, arrows, Fig.

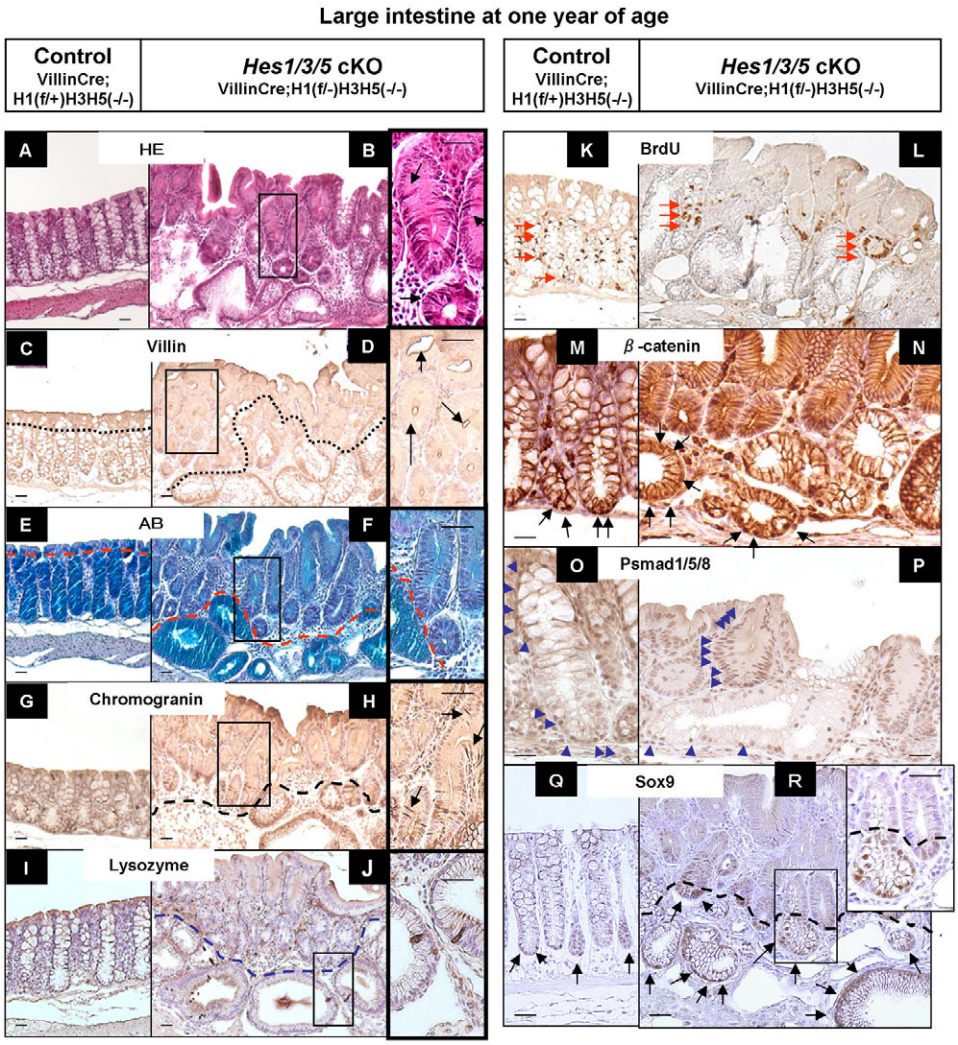

Fig. 5. Defects in the large intestine of *Hes1/3/5* cKO mice at 1 year of age. The large intestines of *Hes1/3/5* cKO and control mice were examined at 1 year of age. (**A**,**B**) Hematoxylin-Eosin staining. Crypts of the large intestine were greatly expanded and formed villus-like structures in *Hes1/3/5* cKO mice (B) as compared with controls (A). (**C**,**D**) Absorptive cells (villin$^+$) were present at the flat surface in controls (C, above dotted line). However, in *Hes1/3/5* cKO mice, the absorptive cell population was remarkably expanded in the inner half of crypts (D, above dotted line, arrows). (**E**,**F**) Goblet cells (Alcian Blue$^+$) formed expanded crypts in their bottom region (below dashed line). (**G**,**H**) The number of enteroendocrine cells (chromogranin$^+$) was increased mainly in the luminal half of the crypts of *Hes1/3/5* cKO mice (H, arrows), as compared with the control (G). (**I**,**J**) Paneth cells (lysozyme$^+$) were not present in the large intestine of control mice (I), but were abundant in *Hes1/3/5* cKO mice (J). (**K**,**L**) BrdU uptake was examined 2 hours after BrdU injection. In control mice, BrdU$^+$ proliferative cells were present within the bottom two-thirds of the crypts (K, arrows), whereas in *Hes1/3/5* cKO mice they were present around the middle region of the crypts (L, arrows). (**M-R**) Immunohistochemical analysis for β-catenin, phosphorylated Smad1/5/8 and Sox9. All three were similarly expressed (arrows and arrowheads) in *Hes1/3/5* cKO mice and controls. Boxed regions are enlarged to the right. Scale bars: 100 μm.

4O). Lgr5$^+$ stem cells were also observed in the middle region of the crypts in *Hes1/3/5* cKO mice, although the number of Lgr5$^+$ stem cells was not noticeably different from that in control mice (supplementary material Fig. S7B, arrow). In these mutant mice, BrdU$^+$ cells migrated not only towards the luminal side but also towards the bottom (Fig. 4G, arrows). Moreover, 96 hours later, BrdU$^+$ cells that migrated upwards had disappeared, whereas those that migrated to the bottom still remained in the crypts (Fig. 4K, arrows). Apoptosis (cleaved caspase 3$^+$ cells) occurred only at the flat surface of the large intestine in control mice (supplementary material Fig. S7C, arrows), but occurred at both the flat surface (black arrows) and the crypt base region (red arrows) in the large intestine of *Hes1/3/5* cKO mice (supplementary material Fig. S7D), probably owing to abnormal bidirectional migration. Thus, in the large intestine of *Hes1/3/5* cKO mice, cell proliferation was significantly reduced although Lgr5$^+$ stem cells were preserved, and mislocalization of stem cells and abnormal migration of differentiated cells were observed.

We next examined the turnover of differentiated cells by multiple BrdU injections. Nine days after multiple BrdU injections, no BrdU$^+$ cells were detectable in the large intestine of control mice (Fig. 4M), indicating that the turnover was very rapid. By contrast, many BrdU$^+$ cells were observed specifically in the cystic crypt bottom of *Hes1/3/5* cKO mice (Fig. 4N, below dotted red line), suggesting that the progeny cells migrating towards the bottom had a slow turnover. These results indicated that the survival of differentiated cells is enhanced in the large intestine of *Hes1/3/5* cKO mice.

Progressive alteration in the large intestine of *Hes1/3/5* cKO mice

In the large intestine of 1-year-old *Hes1/3/5* cKO mice, the number of villin$^+$ absorptive cells was noticeably increased and they expanded into the luminal side, forming villus-like structures with a morphology reminiscent of the small intestine (Fig. 5B,D, above dotted line), whereas the large intestine in control animals did not form such structures (Fig. 5A,C). Goblet cells (Alcian Blue$^+$) were also noticeably increased in number, but they were present in the bottom side of *Hes1/3/5* cKO mice (Fig. 5E,F). Enteroendocrine cells (chromogranin$^+$) were overproduced in the luminal side, and Paneth cells (lysozyme$^+$) were ectopically present in the bottom side of the large intestine of *Hes1/3/5* cKO mice (Fig. 5G-J). Proliferating cells were present in the bottom half of the large intestine of control mice (Fig. 5K, arrows), whereas they were mispositioned around the middle region of the crypt in *Hes1/3/5* cKO mice (Fig. 5L, arrows), as observed at 2 months of age. These results suggest that the large intestine of *Hes1/3/5* cKO mice was progressively altered in morphology and became somewhat similar to small intestine, although their detailed structures were different.

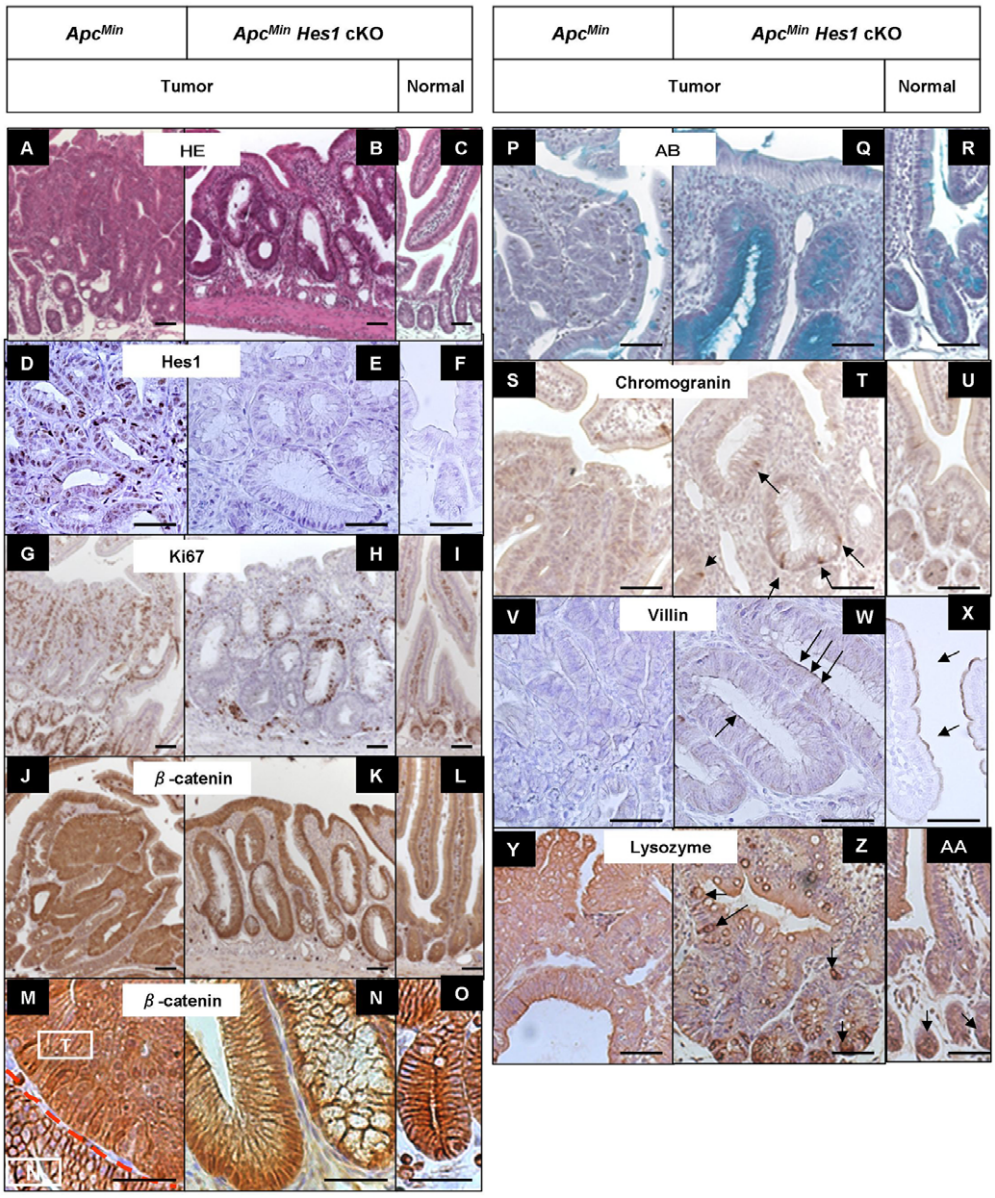

Fig. 6. Induction of differentiation of tumor cells in *Apc^Min^* mice by inactivation of *Hes1*. Histological analysis of tumor regions of *Apc^Min^;Villin-Cre;Hes1^flox/+^* (*Apc^Min^* mice, A,D,G,J,M,P,S,V,Y) and *Apc^Min^;Villin-Cre;Hes1^flox/–^* (*Apc^Min^;Hes1* cKO mice, B,E,H,K,N,Q,T,W,Z) and of non-tumor regions of *Apc^Min^;Hes1* cKO mice (C,F,I,L,O,R,U,X,AA). (**A-C**) Hematoxylin-Eosin staining. Similar to *Apc^Min^* mice (A), *Apc^Min^;Hes1* cKO mice developed many adenoma polyps (B). (**D-F**) Hes1 was highly expressed in tumor cells of *Apc^Min^* mice (D) but not in *Apc^Min^;Hes1* cKO mice (E,F). (**G-I**) Most tumor cells of *Apc^Min^* mice were proliferating (Ki67^+^, G), whereas only subsets of tumor cells were proliferating in *Apc^Min^;Hes1* cKO mice (Ki67^+^, H). (**J-O**) Nuclear β-catenin was similarly expressed by tumor cells in *Apc^Min^* mice (J,M; boxes T and N indicate tumor and normal tissues, respectively) and in *Apc^Min^;Hes1* cKO mice (K,N). (**P-R**) Alcian Blue staining showed that there were no goblet cells present in tumors of *Apc^Min^* mice (P) but many in the tumors of *Apc^Min^;Hes1* cKO mice (Q). (**S-AA**) Immunohistochemical analysis showed that there were virtually no enteroendocrine (chromogranin^+^), absorptive (villin^+^) or Paneth (lysozyme^+^) cells in tumors of *Apc^Min^* mice (S,V,Y) but many in the tumors of *Apc^Min^;Hes1* cKO mice (T,W,Z, arrows). Non-tumor regions of *Apc^Min^;Hes1* cKO mice were normal (C,F,I,L,O,R,U,X,AA). Scale bars: 100 μm.

Because the distribution of differentiated epithelial cells was altered in *Hes1/3/5* cKO mice, we analyzed the Wnt and BMP signaling pathways, which antagonistically regulate the lineage commitment of intestinal stem cells (Scoville et al., 2008). The distributions of nuclear β-catenin, a Wnt signaling effector, and of phosphorylated Smad1/5/8, a BMP signaling effector, were very similar in control and *Hes1/3/5* cKO mice (Fig. 5M,N, arrows; Fig. 5O,P, arrowheads), suggesting that no significant alteration of the Wnt and BMP pathways had occurred in the mutants. Because the large intestine also shows the small intestine-like morphology in the absence of *Sox9* (Bastide et al., 2007), we examined Sox9 expression. Sox9 was similarly expressed in the bottom regions of both control and *Hes1/3/5* cKO mice at 2 months (Fig. 3M,N, arrows, and supplementary material Fig. S5A,B) and 1 year (Fig. 5Q,R, arrows) of age. However, some of the mispositioned proliferating cells in *Hes1/3/5* cKO mice, which were located at the luminal side of the large intestine (Fig. 5L), seemed to lose Sox9 expression, suggesting that these Sox9-negative proliferating cells might contribute to the small intestine-like morphology.

Decreased proliferation and increased differentiation of tumor cells in the absence of *Hes1*

Finally, to determine the role of *Hes1* in intestinal tumor development, we crossed *Apc^Min^* mice with *Hes1* cKO mice. Tumors developed in the intestine of *Apc^Min^* mice by loss-of-function mutation of *Apc* (supplementary material Fig. S8A-E), and nuclear β-catenin was stabilized in these tumor cells (Fig. 6A,J,M). These tumor cells also expressed a high level of Hes1 (Fig. 6D). In *Apc^Min^;Hes1* cKO mice, in which *Hes1* was almost completely inactivated (Fig. 6E,F and supplementary material Fig. S8F,G), tumors also developed and nuclear β-catenin was stabilized in such tumor cells (Fig. 6B,K,N). However, whereas many tumor cells proliferated (Ki67^+^) in *Apc^Min^* mice (Fig. 6G and supplementary material Fig. S8J), only subsets of them were positive for Ki67 in *Apc^Min^;Hes1* cKO mice (Fig. 6H and supplementary material Fig. S8K), indicating that many tumor cells exited the cell cycle in the absence of *Hes1*. Furthermore, there were many differentiated goblet cells, enteroendocrine cells, absorptive cells and Paneth cells

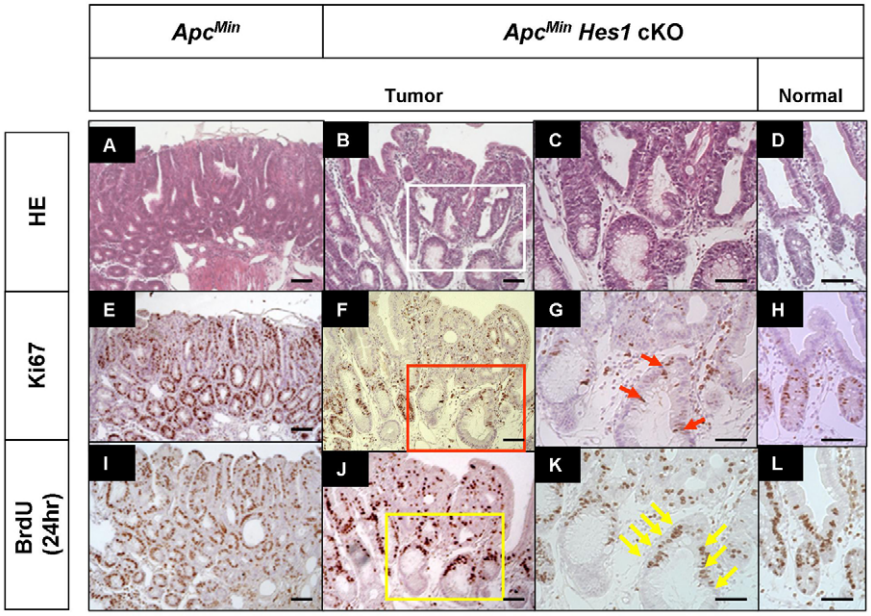

Fig. 7. Cell cycle exit of tumor cells in *Apc*^{Min} mice by inactivation of *Hes1*. (**A-L**) Histological analysis of tumor regions of *Apc*^{Min};*Villin-Cre*;*Hes1*$^{flox/+}$ (*Apc*^{Min} mice, A,E,I) and *Apc*^{Min};*Villin-Cre*;*Hes1*$^{flox/-}$ (*Apc*^{Min};*Hes1* cKO mice, B,C,F,G,J,K) and non-tumor regions of *Apc*^{Min};*Hes1* cKO mice (D,H,L). Boxed regions in B,F,J are enlarged in C,G,K, respectively. F,G and J,K are serial sections. Histological analysis by Hematoxylin-Eosin staining (A-D) and immunohistochemical analysis (E-L) of polyp sections 24 hours after single BrdU injections. The number of proliferating cells (Ki67$^+$) decreased noticeably in *Apc*^{Min};*Hes1* cKO mice (F,G, arrows), compared with *Apc*^{Min} mice (E). Most of the BrdU$^+$ cells in *Apc*^{Min} mice expressed Ki67 (E,I), indicating that the tumor cells continued to proliferate. By contrast, most of the BrdU$^+$ cells in *Apc*^{Min};*Hes1* cKO mice did not express Ki67 (F,G,J,K), indicating that many tumor cells had exited the cell cycle. Note that Ki67$^+$ (G, arrows) and BrdU$^+$ (K, arrows) cells were mostly distinct from each other. Scale bars: 100 μm.

in the tumor regions of *Apc*^{Min};*Hes1* cKO mice (Fig. 6Q,T,W,Z, arrows, and supplementary material Fig. S8I) as observed in non-tumor regions (Fig. 6R,U,X,AA), whereas there were virtually no such differentiated cells in tumors of *Apc*^{Min} mice (Fig. 6P,S,V,Y and supplementary material Fig. S8H). Math1 and Ngn3, which induce secretory and enteroendocrine cell development, respectively, were also upregulated in the tumor regions of *Apc*^{Min};*Hes1* cKO mice as compared with *Apc*^{Min} mice (supplementary material Fig. S9). These results suggest that, in the absence of *Hes1*, tumor cells do not continue to proliferate but instead differentiate into postmitotic intestinal cells.

To clarify this idea, we examined the proliferation activity of tumor cells 24 hours after BrdU administration. In *Apc*^{Min} mice, almost all BrdU$^+$ tumor cells were positive for Ki67 even 24 hours after BrdU administration (Fig. 7A,E,I), suggesting that these tumor cells continued to proliferate. By contrast, in *Apc*^{Min};*Hes1* cKO mice, the numbers of BrdU$^+$ or Ki67$^+$ tumor cells were significantly reduced compared with *Apc*^{Min} mice (Fig. 7B,C,F,G,J,K), suggesting that most proliferating tumor cells differentiated into postmitotic cells in the absence of *Hes1*. In non-tumor regions of *Apc*^{Min};*Hes1* cKO mice, cell proliferation and differentiation were unaffected by *Hes1* KO (Fig. 6C,F,I,L,O,R,U,X,AA and Fig. 7D,H,L).

Apc^{Min} mice were also crossed with *Hes1/3/5* cKO mice. In these mice, there were many differentiated cells, such as goblet cells (supplementary material Fig. S10D), although intestinal adenomas expressed nuclear β-catenin at a high level, similar to that observed in *Apc*^{Min} mice (supplementary material Fig. S10A,B,G,H). In *Apc*^{Min};*Hes1/3/5* cKO mice, only subsets of tumor cells were positive for Ki67 (supplementary material Fig. S10F). However, the tumor phenotypes of *Apc*^{Min};*Hes1/3/5* cKO mice were very similar to those of *Apc*^{Min};*Hes1* cKO mice, suggesting that *Hes1* is dominant for tumor progression.

Because Hes1 was not expressed in *Apc*^{Min};*Hes1* cKO mice during tumor formation, intestinal adenoma formation might be incomplete compared with that in *Apc*^{Min} mice. To examine the role of *Hes1* in fully developed intestinal adenomas, we induced *Hes1* KO in adult *Apc*^{Min} mice. We crossed *Hes1* flox mice with Ah-Cre mice, which express Cre under the control of the cytochrome P4501A1 (*Cyp1a1*) promoter (Campbell et al., 1996; Ireland et al., 2004). In Ah-Cre mice, Cre-dependent recombination is induced in the intestinal epithelium as well as in the liver parenchyma, the pancreas and the esophagus after β-naphthoflavone administration (supplementary material Fig. S11) (Ireland et al., 2004). *Ah-Cre*;*Hes1*$^{flox/-}$;*Apc*^{Min} mice were treated with β-naphthoflavone at 3 months of age, when intestinal adenomas had already developed. Similar to the tumor cells in the *Apc*^{Min};*Hes1* cKO mice described above, most tumor cells that expressed a high level of nuclear β-catenin became negative for Ki67 when Hes1 expression was lost (Fig. 8, below dashed line). These results indicate that Hes1 plays an important role in the maintenance of proliferating tumor cells, and that inhibition of Hes1 activity induces cell cycle exit and differentiation of intestinal tumor cells without affecting normal regions.

DISCUSSION

Hes genes promote cell proliferation and negatively regulate intestinal secretory cell development

In this study, we examined the roles of Hes genes in the regulation of intestinal development and homeostasis by analyzing Hes KO mice. In previous reports, the small intestine of *Hes1* KO neonatal mice showed overproduction of secretory cells (Jensen et al., 2000; Suzuki et al., 2005). However, it was unclear whether *Hes1* is similarly important for regulating postnatal development and homeostasis of intestinal cells, as *Hes1* KO mice die soon after birth. It was previously shown that, in adult *Rbpj* cKO mice and adult wild-type mice treated with a γ-secretase inhibitor, all proliferating cells exit the cell cycle and differentiate into goblet cells (van Es et al., 2005a; Riccio et al., 2008). We found that *Hes1* cKO mice only displayed an increase in the number of secretory cells during a neonatal stage, whereas *Hes1/3/5* cKO mice displayed a reduction in the number of proliferating cells as well as an increase in the number of secretory cells. In these mutant mice, in addition to goblet cells, the number of enteroendocrine cells was noticeably increased. Furthermore, Paneth cells were observed in neither the neonatal small intestine nor the large intestine, whereas they appeared in these regions of *Hes1/3/5* cKO

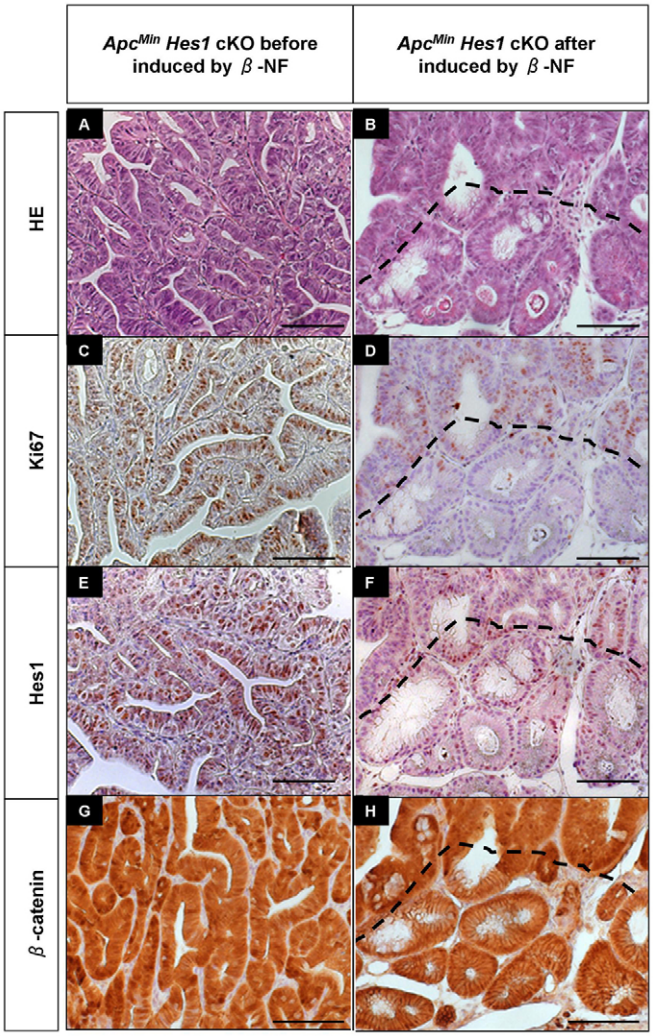

Fig. 8. Differentiation of tumor cells in *Ah-Cre;Hes1*$^{flox/-}$*;Apc*^{Min} mice after β-naphthoflavone administration. Tumor cells in *Ah-Cre;Hes1*$^{flox/-}$*;Apc*^{Min} mice were examined before (A,C,E,G) or after (B,D,F,H) β-naphthoflavone administration. (**A**,**B**) Hematoxylin-Eosin staining. (**C**,**D**) Before β-naphthoflavone administration there were many proliferating cells (C, Ki67^{+}). After β-naphthoflavone administration, the number of proliferating cells was significantly reduced (D, below dashed line). (**E**,**F**) Before β-naphthoflavone administration, most tumor cells expressed Hes1 at high levels (E). After β-naphthoflavone administration, many tumor cells lost Hes1 expression (F, below dashed line). (**G**,**H**) Nuclear β-catenin was expressed similarly before and after β-naphthoflavone administration. Scale bars: 100 μm.

mice. These results indicate that all Hes genes negatively regulate the development of all types of secretory cells. Importantly, *Hes1/3/5* cKO mice continued to display the same abnormality in the adult, whereas *Hes1* cKO mice lost this abnormality in the adult, probably because *Hes3* and *Hes5* compensate for the *Hes1* deficiency. Thus, *Hes1* is dominant during embryonic and neonatal stages, whereas all Hes genes cooperatively regulate adult homeostasis.

In both *Hes1* cKO and *Hes1/3/5* cKO mice there were still many Lgr5^{+} stem cells, and only subsets of them differentiated into goblet cells, indicating that the outcomes of inactivation of Hes genes are different from the effects of inactivation of Notch signaling. Although Hes genes are required for the proliferation of intestinal progenitor cells, they are not essential for the maintenance of stem cells, suggesting that other Notch effectors might compensate for Hes genes in the maintenance of stem cells. These results also suggest that, in the Notch signaling pathway, genes other than Hes genes mainly regulate the production of goblet cells over other types of cells. Hes genes seem to be essential for the proliferation of transit-amplifying or progenitor cells and for the secretory versus absorptive cell fate decision during intestinal development and homeostasis.

Hes genes keep stem cells in the correct position on the crypt-villus axis

Intestinal stem cells reside at the crypt bottom (Barker et al., 2007; Barker et al., 2008; Sangiorgi and Capecchi, 2008): stem cells exist between and just above Paneth cells in the small intestine and between progenitors of goblet cells in the large intestine. In *Hes1/3/5* cKO mice, proliferating cells were reduced in number and their position was changed. This defect was particularly evident in the large intestine of *Hes1/3/5* cKO mice, in which the lower parts of the crypts were gradually expanded. Although normal progeny cells only migrated towards the lumen surface, the progeny of mutant stem/progenitor cells moved along the crypt-villus axis not only towards the surface lumen but also towards the crypt bottom in the large intestine. In addition, the cells that migrated abnormally to the crypt base displayed a lower turnover than normal intestinal cells, which probably led to expansion of the mutant crypts. It is likely that the abnormal migration and expansion of crypts lead to the mislocalization of stem/progenitor cells.

Mislocalization of stem/progenitor cells could in turn lead to abnormal cell differentiation. In the intestine, signaling factors such as Wnt and BMP form gradients along the crypt-villus axis to regulate stem/progenitor cell differentiation (Radtke and Clevers, 2005; Crosnier et al., 2006; Scoville et al., 2008). Wnt signaling activity is highest at the bottom of crypts and gradually decreases along the crypt-villus axis, whereas the activity of BMP signaling shows the opposite gradient (Kosinski et al., 2007; Scoville et al., 2008), and BMP signaling and Wnt signaling antagonize each other (He et al., 2004). Normally, Paneth cells reside at the crypt bottom, receive Wnt signaling and express EphB3, a downstream target for Wnt signaling, which keeps Paneth cells at the crypt bottom (Batlle et al., 2002). In the small intestine of *Hes1/3/5* cKO mice, however, some Paneth cells did not remain at the crypt bottom but migrated towards the luminal side along the crypt-villus axis. Transgenic mice expressing the secreted Wnt inhibitor Dkk1 (Villin-Dkk1), and intestine-specific cKO mice of the Wnt receptor frizzled 5 (Fzd5), display mislocalization of Paneth cells resulting from a decrease in Wnt signaling activity (Pinto et al., 2003; van Es et al., 2005b). In *Hes1/3/5* cKO mice, Paneth cells remaining at the crypt bottom showed nuclear β-catenin expression and also expressed EphB3, whereas mispositioned Paneth cells showed neither nuclear β-catenin staining nor EphB3 expression, similar to the defects observed in Villin-Dkk1 and *Fzd5* cKO mice. It is likely that some differentiating Paneth cells cannot receive proper Wnt signaling owing to changes in the position of the stem/progenitor cells in *Hes1/3/5* cKO mice and consequently lose EphB3 expression, which further enhances the mislocalization of Paneth cells.

The large intestine also showed abnormal cell differentiation in *Hes1/3/5* cKO mice 1 year after birth. In the mutant large intestine, stem cells were located around the middle region of the crypt.

Absorptive cells and enteroendocrine cells were distributed above the stem cells, whereas goblet cells and Paneth cells were located below them. In the adult intestine, Wnt signaling regulates the development of goblet cells and Paneth cells via Sox9 (Ireland et al., 2004; Bastide et al., 2007; Mori-Akiyama et al., 2007; Wang et al., 2007), whereas BMP signaling mainly controls the development of enteroendocrine cells (Auclair et al., 2007). Therefore, it is likely that, in the large intestine of *Hes1/3/5* cKO mice, progenitors migrating to the lumen lose Sox9 expression and differentiate into enteroendocrine cells as well as absorptive cells, whereas secretory progenitors moving to the crypt base differentiate into Paneth cells or goblet cells under the control of Wnt signaling via Sox9.

Thus, Hes genes not only control the size of the proliferating cell population, but also keep stem cells in the correct position on the crypt-villus axis, thereby allowing stem cells to receive signaling molecules and to differentiate properly into epithelial cells.

Hes1 is required for maintenance of the undifferentiated state of tumor cells

We also showed that *Hes1* plays an important role in maintaining the undifferentiated state of intestinal tumor cells. In the absence of *Hes1*, many tumor cells exited the cell cycle and differentiated into postmitotic epithelial cells, even though these cells showed stabilization of nuclear β-catenin expression. A recent study showed that Hes1 expression is directly regulated by Notch and Wnt/β-catenin signaling (Peignon et al., 2011), suggesting that these pathways converge on Hes1.

It was previously shown that inhibition of Notch signaling by a γ-secretase inhibitor induced differentiation of adenoma cells into goblet cells, suggesting that Notch signaling might be a promising target for colorectal cancer therapy. However, γ-secretase inhibitors also caused all proliferating cells within the crypts of healthy intestinal regions to differentiate into goblet cells throughout the small and large intestines (Wong et al., 2004; van Es et al., 2005a), which could cause severe diarrhea and malabsorption. By contrast, inactivation of *Hes1* had no apparent effect on cell proliferation and differentiation in the crypts of non-tumor regions, probably because other factors compensate for *Hes1* deficiency. Thus, Hes1 would be a better target to induce the differentiation of tumor cells. Recently, selective anti-Notch receptor antibodies were developed and shown to inhibit the growth of human colon cancer cells in xenotransplantation models (Wu et al., 2010). However, it remains to be investigated whether each Notch-specific antibody can repress tumor growth in Apc^{Min} mice, as *Notch1* and *Notch2* are functionally redundant (Riccio et al., 2008) and because Hes1 expression remains after treatment with Notch1- or Notch2-specific antibody in the adult intestine (Wu et al., 2010).

Our study revealed the roles of Hes genes in the regulation of intestinal development and homeostasis. Hes genes control not only the proliferation and differentiation of stem/progenitor cells but also their positions, so that these cells properly receive and respond to signaling molecules. We also showed that inactivation of *Hes1* alone is sufficient to reduce tumor cell proliferation and induce the differentiation of tumor cells into all types of intestinal epithelial cells. Importantly, inactivation of *Hes1* does not affect the proliferation or differentiation of cells within normal crypts in adult animals, raising the possibility that *Hes1* might be a good target for a therapy that aims to induce tumor cell differentiation.

Acknowledgements
We thank Philippe Soriano and C. Roland Wolf for materials.

Funding
This work was supported by Japan Society for the Promotion of Science (JSPS) Grants-in-aid for Scientific Research [21229009, 23590937, 22790642]; and Health and Labor Sciences Research Grants for Research on Intractable Disease, and Research on Hepatitis from the Ministry of Health, Labor and Welfare, Japan.

Competing interests statement
The authors declare no competing financial interests.

Supplementary material
Supplementary material available online at
http://dev.biologists.org/lookup/suppl/doi:10.1242/dev.069070/-/DC1

References

Auclair, B. A., Benoit, Y. D., Rivard, N., Mishina, Y. and Perreault, N. (2007). BMP morphogenetic protein signaling is essential for terminal differentiation of the intestinal secretory cell lineage. *Gastroenterology* **133**, 887-896.

Barker, N., van Es, J. H., Kuipers, J., Kujala, P., van den Born, M., Cozijnsen, M., Haegebarth, A., Korving, J., Begthel, H., Peters, P. J. and Clevers, H. (2007). Identification of stem cells in small intestine and colon by marker gene Lgr5. *Nature* **449**, 1003-1007.

Barker, N., van de Wetering, M. and Clevers, H. (2008). The intestinal stem cells. *Nat. Genet.* **40**, 915-920.

Bastide, P., Darido, C., Pannequin, J., Kist, R., Robine, S., Marty-Double, C., Bibeau, F., Scherer, G., Joubert, D., Hollande, F. et al. (2007). Sox9 regulates cell proliferation and is required for Paneth cell differentiation in the intestinal epithelium. *J. Cell Biol.* **178**, 635-648.

Batlle, E., Henderson, J. T., Beghtel, H., van den Born, M. M., Sancho, E., Huls, G., Meeldijk, J., Robertson, J., van de Wetering, M., Pawson, T. and Clevers, H. (2002). Beta-catenin and TCF mediate cell positioning in the intestinal epithelium by controlling the expression of EphB/ephrinB. *Cell* **111**, 251-263.

Bienz, M. and Clevers, H. (2000). Linking colorectal cancer to Wnt signaling. *Cell* **103**, 311-320.

Campbell, S. J., Carlotti, F., Hall, P. A., Clark, A. J. and Wolf, C. R. (1996). Regulation of the CYP1A1 promoter in transgenic mice: an exquisitely sensitive on-off system for cell specific gene regulation. *J. Cell Sci.* **109**, 2619-2625.

Crosnier, C., Stamataki, D. and Lewis, J. (2006). Organizing cell renewal in the intestine: stem cells, signals and combinatorial control. *Nat. Rev. Genet.* **7**, 349-359.

el Marjou, F., Janssen, K. P., Chang, B. H., Li, M., Hindie, V., Chan, L., Louvard, D., Chambon, P., Metzger, D. and Robine, S. (2004). Tissue-specific and inducible Cre-mediated recombination in the gut epithelium. *Genesis* **39**, 186-193.

Fernández-Majada, V., Aguilera, C., Villanueva, A., Vilardell, F., Robert-Moreno, A., Aytés, A., Real, F. X., Capella, G., Mayo, M. W., Espinosa, L. and Bigas, A. (2007). Nuclear IKK activity leads to dysregulated notch-dependent gene expression in colorectal cancer. *Proc. Natl. Acad. Sci. USA* **104**, 276-281.

Fre, S., Huyghe, M., Mourikis, P., Robine, S., Louvard, D. and Artavanis-Tsakonas, S. (2005). Notch signals control the fate of immature progenitor cells in the intestine. *Nature* **435**, 964-968.

Fre, S., Pallavi, S. K., Huyghe, M., Laé, M., Janssen, K. P., Robine, S., Artavanis-Tsakonas, S. and Louvard, D. (2009). Notch and Wnt signals cooperatively control cell proliferation and tumorigenesis in the intestine. *Proc. Natl. Acad. Sci. USA* **106**, 6309-6314.

Hatakeyama, J., Bessho, Y., Katoh, K., Ookawara,S., Fujioka, M., Guillemot, F. and Kageyama, R. (2004). Hes genes regulate size, shape and histogenesis of the nervous system by control of the timing of neural stem cell differentiation. *Development* **131**, 5539-5550.

He, X. C., Zhang, J., Tong, W. G., Tawfik, O., Ross, J., Scoville, D. H., Tian, Q., Zeng, X., He, X., Wiedemann, L. M. et al. (2004). BMP signaling inhibits intestinal stem cell self-renewal through suppression of Wnt-β-catenin signaling. *Nat. Genet.* **36**, 1117-1121.

Imayoshi, I., Ohtsuka, T., Metzger, D., Chanbon, P. and Kageyama, R. (2006). Temporal regulation of Cre recombinase activity in neural stem cells. *Genesis* **44**, 233-238.

Imayoshi, I., Shimogori, T., Ohtsuka, T. and Kageyama, R. (2008). Hes genes and neurogenin regulate non-neural versus neural fate specification in the dorsal telencephalic midline. *Development* **135**, 2531-2541.

Ireland, H., Kemp, R., Houghton, C., Howard, L., Clarke, A. R., Sansom, O. J. and Winton, D. J. (2004). Inducible Cre-mediated control of gene expression in murine gastrointestinal tract: effect of loss of β-catenin. *Gastroenterology* **126**, 1236-1246.

Ishibashi, M., Ang, S. L., Shiota, K., Nakanishi, S., Kageyama, R. and Guillemot, F. (1995). Targeted disruption of mammalian hairy and Enhancer of split homolog-1 (HES-1) leads to up-regulation of neural helix-loop-helix factors,

premature neurogenesis, and severe neural tube defects. *Genes Dev.* **9**, 3136-3148.
Jenny, M., Uhl, C., Roche, C., Duluc, I., Guillermin, V., Guillemot, F., Jensen, J., Kedinger, M. and Gradwohl, G. (2002). Neurogenin3 is differentially required for endocrine cell fate specification in the intestinal and gastric epithelium. *EMBO J.* **21**, 6338-6347.
Jensen, J., Pedersen, E. E., Galante, P., Hald, J., Heller, R. S., Ishibashi, M., Kageyama, R., Guillemot, F., Serup, P. and Madsen, O. D. (2000). Control of endodermal endocrine development by Hes-1. *Nat. Genet.* **24**, 36-44.
Kageyama, R., Ohtsuka, T. and Kobayashi, T. (2007). The Hes gene family: repressors and oscillators that orchestrate embryogenesis. *Development* **134**, 1243-1251.
Kayahara, T., Sawada, M., Takaishi, S., Fukui, H., Seno, H., Fukuzawa, H., Suzuki, K., Hiai, H., Kageyama, R., Okano, H. and Chiba, T. (2003). Candidate markers for stem and early progenitor cells, Musashi-1 and Hes1, are expressed in crypt base columnar cells of mouse small intestine. *FEBS Lett.* **535**, 131-135.
Kopinke, D., Brailsford, M., Shea, J. E., Leavitt, R., Scaife, C. L. and Murtaugh, L. C. (2011). Lineage tracing reveals the dynamic contribution of Hes1+ cells to the developing and adult pancreas. *Development* **138**, 431-441.
Kosinski, C., Li, V. S., Chan, A. S., Zhang, J., Ho, C., Tsui, W. Y., Chan, T. L., Mifflin, R. C., Powell, D. W., Yuen, S. T. et al. (2007). Gene expression patterns of human colon tops and basal crypts and BMP antagonists as intestinal stem cell niche factors. *Proc. Natl. Acad. Sci. USA* **104**, 15418-15423.
Kunisato, A., Chiba, S., Nakagami-Yamaguchi, E., Kumano, K., Saito, T., Masuda, S., Yamaguchi, T., Osawa, M., Kageyama, R., Nakauchi, H. et al. (2003). HES-1 preserves purified hematopoietic stem cells ex vivo and accumulates side population cells in vivo. *Blood* **101**, 1777-1783.
Madison, B. B., Dunbar, L., Qiao, X. T., Braunstein, K., Braunstein, E. and Gumucio, D. L. (2002). cis elements of the villin gene control expression in restricted domains of the vertical (crypt) and horizontal (duodenum, cecum) axes of the intestine. *J. Biol. Chem.* **277**, 33275-33283.
Mori-Akiyama, Y., van den Born, M., van Es, J. H., Hamilton, S. R., Adams, H. P., Zhang, J., Clevers, H. and de Crombrugghe, B. (2007). SOX9 is required for the differentiation of paneth cells in the intestinal epithelium. *Gastroenterology* **133**, 539-546.
Moser, A. R., Pitot, H. C. and Dove, W. F. (1990). A dominant mutation that predisposes to multiple intestinal neoplasia in the mouse. *Science* **247**, 322-324.
Ohtsuka, T., Ishibashi, M., Gradwohl, G., Nakanishi, S., Guillemot, F. and Kageyama, R. (1999). Hes1 and Hes5 as notch effectors in mammalian neuronal differentiation. *EMBO J.* **18**, 2196-2207.
Peignon, G., Durand, A., Cacheux, W., Ayrault, O., Terris, B., Laurent-Puig, P., Shroyer, N. F., Van Seuningen, I., Honjo, T., Perret, C. and Romagnolo, B. (2011). Complex interplay between β-catenin signalling and Notch effectors in intestinal tumorigenesis. *Gut* **60**, 166-176.
Pinto, D., Gregorieff, A., Begthel, H. and Clevers, H. (2003). Canonical Wnt signals are essential for homeostasis of the intestinal epithelium. *Genes Dev.* **17**, 1709-1713.
Radtke, F. and Clevers, H. (2005). Self-renewal and cancer of the gut: two sides of a coin. *Science* **307**, 1904-1909.
Riccio, O., van Gijn, M. E., Bezdek, A. C., Pellegrinet, L., van Es, J. H., Zimber-Strobl, U., Strobl, L. J., Honjo, T., Clevers, H. and Radtke, F. (2008). Loss of intestinal crypt progenitor cells owing to inactivation of both Notch1 and Notch2 is accompanied by derepression of CDK inhibitors p27Kip1 and p57Kip2. *EMBO Rep.* **9**, 377-383.
Rodilla, V., Villanueva, A., Obrador-Hevia, A., Robert-Moreno, A., Fernández-Majada, V., Grilli, A., López-Bigas, N., Bellora, N., Albà, M. M., Torres, F. et al. (2009). Jagged1 is the pathological link between Wnt and Notch pathways in colorectal cancer. *Proc. Natl. Acad. Sci. USA* **106**, 6315-6320.
Sangiorgi, E. and Capecchi, M. R. (2008). Bmi1 is expressed in vivo in intestinal stem cells. *Nat. Genet.* **40**, 915-920.
Scoville, D. H., Sato, T., He, X. C. and Li, L. (2008). Current view: intestinal stem cells and signaling. *Gastroenterology* **134**, 849-864.
Shimojo, H., Ohtsuka, T. and Kageyama, R. (2008). Oscillations in notch signaling regulate maintenance of neural progenitors. *Neuron* **58**, 52-64.
Soriano, P. (1999). Generalized lacZ expression with the ROSA26 Cre reporter strain. *Nat. Genet.* **21**, 70-71.
Stanger, B. Z., Datar, R., Murtaugh, L. C. and Melton, D. A. (2005). Direct regulation of intestinal fate by Notch. *Proc. Natl. Acad. Sci. USA* **102**, 12443-12448.
Su, L. K., Kinzler, K. W., Vogelstein, B., Preisinger, A. C., Moser, A. R., Luongo, C., Gould, K. A. and Dove, W. F. (1992). Multiple intestinal neoplasia caused by a mutation in the murine homolog of the APC gene. *Science* **256**, 668-670.
Suzuki, K., Fukui, H., Kayahara, T., Sawada, M., Seno, H., Hiai, H., Kageyama, R., Okano, H. and Chiba, T. (2005). Hes1-deficient mice show precocious differentiation of Paneth cells in the small intestine. *Biochem. Biophys. Res. Commun.* **328**, 348-352.
van de Wetering, M., Sancho, E., Verweij, C., de Lau, W., Oving, I., Hurlstone, A., van der Horn, K., Batlle, E., Coudreuse, D., Haramis, A. P. et al. (2002). The beta-catenin/TCF-4 complex imposes a crypt progenitor phenotype on colorectal cancer cells. *Cell* **111**, 241-250.
van Es, J. H., van Gijn, M. E., Riccio, O., van den Born, M., Vooijs, M., Begthel, H., Cozijnsen, M., Robine, S., Winton, D. J., Radtke, F. and Clevers, H. (2005a). Notch/gamma-secretase inhibition turns proliferative cells in intestinal crypts and adenomas into goblet cells. *Nature* **435**, 959-963.
van Es, J. H., Jay, P., Gregorieff, A., van Gijn, M. E., Jonkheer, S., Hatzis, P., Thiele, A., van den Born, M., Begthel, H., Brabletz, T. et al. (2005b). Wnt signaling induces maturation of Paneth cells in intestinal crypts. *Nat. Cell Biol.* **7**, 381-386.
Wang, Y., Giel-Moloney, M., Rindi, G. and Leiter, A. B. (2007). Enteroendocrine precursors differentiate independently of Wnt and form serotonin expressing adenomas in response to active β-catenin. *Proc. Natl. Acad. Sci. USA* **104**, 11328-11333.
Wilson, A. and Radtke, F. (2006). Multiple functions of Notch signaling in self-renewing organs and cancer. *FEBS Lett.* **580**, 2860-2868.
Wong, G. T., Manfra, D., Poulet, F. M., Zhang, Q., Josien, H., Bara, T., Engstrom, L., Pinzon-Ortiz, M., Fine, J. S., Lee, H. J. et al. (2004). Chronic treatment with the gamma-secretase inhibitor LY-411,575 inhibits beta-amyloid peptide production and alters lymphopoiesis and intestinal cell differentiation. *J. Biol. Chem.* **279**, 12876-12882.
Wu, Y., Cain-Hom, C., Choy, L., Hagenbeek, T. J., de Leon, G. P., Chen, Y., Finkle, D., Venook, R., Wu, X., Ridgway, J. et al. (2010). Therapeutic antibody targeting of individual Notch receptors. *Nature* **464**, 1052-1057.
Yang, Q., Bermingham, N. A., Finegold, M. J. and Zoghbi, H. Y. (2001). Requirement of Math1 for secretory cell lineage commitment in the mouse intestine. *Science* **294**, 2155-2158.